ISSN 0511-5728
The West Indian Journal of Engineering
Vol.35, No.1, July 2012, pp.41-50

Edge Water Drive Detection and Movement from Buildup Data in a Gas Reservoir

Jill Marcelle-De Silva[aΨ] and Shireen Mohammed[b]

[a] Petroleum Studies Unit, Department of Chemical Engineering, The University of the West Indies, St Augustine Campus, Trinidad and Tobago, West Indies; E-mail: Jill.Marcelle-DeSilva@sta.uwi.edu

[b] bpTT, Albion Plaza, Queen's Park West, Port of Spain, Trinidad and Tobago, West Indies; E-mail: shireenm1984@yahoo.com

[Ψ] *Corresponding Author*

(Received 29 June 2011; Revised 14 November 2011; Accepted 04 January 2012)

Abstract: *In the development of gas fields, to provide assurance around delivery of production targets that are contractually agreed upon, several surveillance tools are employed to assist with reservoir management. Such tools include permanent down-hole pressure gauges, wet-gas meters, the production logging tool and the reservoir saturation tool. Surveillance data are collated and analysed to provide assurance while at the same time allowing for the maximum recovery of possible reserves. In this study, pressure transient surveillance data from successive pressure buildup tests conducted on two wells, each located in separate gas reservoirs, were collated and analysed. The data showed that the late time boundary responses indicated by the time-lapsed pressure data were characteristic of an encroaching aquifer. Identification of the recovery mechanism allowed for the early identification of recompletions and opportunities for new wells, and demonstrated the importance of pressure transient data as a reservoir surveillance tool.*

Keywords: *Pressure testing, gas reservoir, time-lapsed pressure data, reservoir surveillance*

Nomenclature:

ϕ	=	porosity, fraction
μ_{gi}	=	gas viscosity at initial reservoir pressure, cp
A	=	drainage area, ft^2
BCF	=	Billion standard cubic feet
C_A	=	shape constant or factor for well drainage area
C_s	=	wellbore storage constant
c_{ti}	=	total system compressibility at initial pressure, $psia^{-1}$
D	=	non-Darcy flow constant, D/Mscf
h	=	net formation thickness, ft
k	=	permeability, md
m(p)	=	real gas pseudo pressure, psi^2/cp
$m(p_{wf})$	=	pseudo pressure evaluated at flowing bottomhole pressure, psi^2/cp
$m(p_{ws})$	=	pseudo pressure evaluated at shutin pressure, psi^2/cp
MMSCF	=	Million standard cubic feet
MMSCF/D	=	Million standard cubic feet per day
MMSTB	=	Million stock tank barrels
p	=	pressure, psia
p_b	=	base pressure, psi
p_i	=	initial pressure, psia
p_{wf}	=	flowing bottom-hole pressure, psia
p_{ws}	=	shutin bottom-hole pressure, psia
q_g	=	gas flow rate, MMscf/D
r_e	=	drainage radius, ft
r_w	=	wellbore radius, ft
s'	=	pseudo skin factor, dimensionless
s	=	skin factor, dimensionless
STB/D	=	Stock tank barrels per day
t	=	elapsed time, hours
T	=	temperature, ^oR
t_a	=	pseudotime, hr-psia/cp
t_D	=	dimensionless time
W	=	channel width
z	=	gas deviation factor

SI Metric Conversion Factors:

bbl x 1.589873	E-01	=	m^3
ft x 3.048	E-01	=	m
mile x 1.609344	E+00	=	km
psi x 6.894757	E+00	=	kPa

1. Introduction

The Caribbean's first liquefied natural gas plant (Atlantic LNG), located in Trinidad and Tobago, began operations in 1999. Several oil and gas companies entered into long term contracts, with assurances of a continuous and sufficient supply of gas from the oil and gas fields, offshore Trinidad.

Several of these fields are located in the Columbus basin. This is a rich depositional centre which extends from Venezuela to southeast Trinidad (Lumsden et al., 2002; Jemmott, 2005). Over 20000 feet of sediments, deposited by the Oronico River System, created reservoirs which contain hydrocarbons trapped against northwest-southeast trending faults. The sandstone reservoirs exhibit high porosities (20 to > 30%) and permeabilities (10 to > 1,000 mD), and are 100 ft to several hundred feet in thickness.

To meet the ever increasing contractual demands,

well designs were changed to produce high rate gas wells (75 to >200 MMSCFD) (Lumsden et al., 2002). Drilling and completing these high rate gas wells, have led to several benefits including the reduction in the well count and associated reduction in capital and operating costs. This however has led to accelerated depletion of the reservoirs, and in conjunction with a poor understanding of reservoir behaviour, supply can become jeopardised.

When available data indicated that several of the reservoirs in the fields were in communication with aquifers, there were concerns surrounding early water breakthrough in producing wells, high residual gas saturations and abandonment pressures, and water handling capability of the surface facilities. To address these concerns, several surveillance tools were employed to allow for close monitoring of reservoir and well performance (Jemmott, 2005; Samsundar et al., 2007; Jemmott et al., 2008). Permanent and temporary downhole pressure gauges are used to provide data to assess reservoir size, production mechanism, deliverability forecasting and wellbore damage. Cased-hole logging tools such as the reservoir saturation tool (RST) are used to track the movement of fluid contacts; the production logging tool (PLT) is used to identify producing intervals and fluid types; permanent acoustic sand monitoring devices are used to minimize the risk of sand control failure; and wet-gas rate meters provide information on gas, condensate and water production rates.

One field, which provides gas to the ALNG plant, is 50 miles off the southeast coast of Trinidad in the Columbus basin, where water depths range from 200 to 300 ft (see Figure 1). In this study, an example of the use of time lapsed pressure transient data from this field to provide well and reservoir surveillance is demonstrated. Pressure buildup (PBU) tests were analysed to provide information on reservoir boundaries, drive mechanism, total skin factor and permeability.

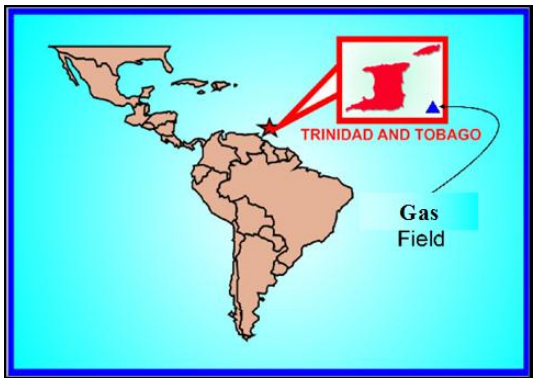

Figure 1. Field Location

2. Field Overview

The field of study is a laterally extensive faulted anticlinal structure (see Figure 2), and is dissected by several normal faults that separate the field into 7 major fault blocks (Mohammed, 2010). The hydrocarbon bearing formations in the field of study are comprised of marine sands and shales sourced from the Orinoco River delta system, located to the west of Trinidad.

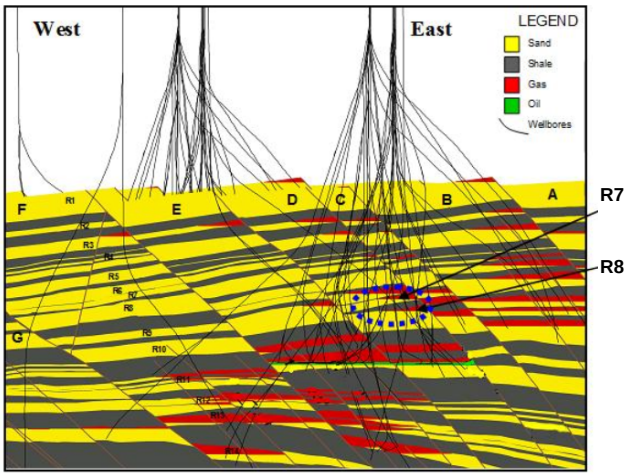

Figure 2. Schematic of Field Cross Section Showing the Locations of the R7 and R8 Sands in Fault Block D

The reservoir system consists of a sequence of seventeen (17) gas bearing sands over a development area of approximately 10,000 acres. All of the hydrocarbon traps in the field are formed by three-way dip closure against the faults. The complex nature of the stacked reservoirs created the challenge of ensuring maximum recoverable reserves, while maintaining production targets which were contractually agreed with ALNG. A surveillance plan was therefore essential.

Reservoirs at depths of less than 10,000 ft are easily identifiable as excellent quality, coarsening upward, blocky reservoir units that are correlative across fault blocks throughout the field. Porosities are in excess of 30% and permeabilities are in the darcy range. In contrast, the sands deeper than 10,000 ft are of poorer reservoir quality. Available data indicate that most of the gas reservoirs are in communication with large aquifers.

This report focuses on two of the gas reservoirs i.e. R7 and R8 located in Fault Block 'D', and at depths in excess of 10,000 ft.

The R7 sand was penetrated by eight wells. As shown in Figure 3, it is elongated and demarcated to the east and west by major faults, and the well penetrations suggest a uniform gas-water contact (GWC) across the entire sand. The single gas production well from the R7 sand in Fault Block 'D', i.e. W1, is located in the southeast section of the block. In this area, the water column gets thicker and as a result, any aquifer encroachment should be through an edge drive

mechanism from the south-east. W1 was thus completed as a cased-hole gravel pack (CHGP) completion with a 37 ft true vertical depth (TVD) stand-off from the original GWC. At target depth (TD) the well's deviation was 23.20º. Petrophysical evaluation provided estimates of net to gross sand thickness ratio of 92.9%, porosity (ϕ) of 24%, and water saturation (S_w) of 26%. Volumetric analysis indicated that the original gas in place (OGIP) was 106.5 BCF. The condensate yield was approximately 7.3 STB/MMSCF, with a gravity of 51º API.

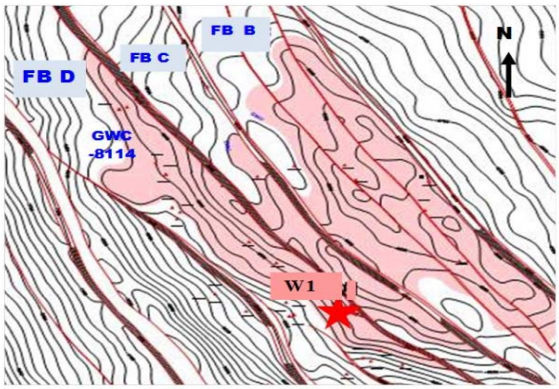

Figure 3. Depth Structure Map for R7 Showing W1 in FB D

Seven wells penetrated the R8 reservoir in Fault Block 'D' (see Figure 4). It is showed that petrophysical evaluations provided estimates of 83.8%, 18% and 28 % for net to gross sand thickness ratio, ϕ and S_w, respectively. Volumetric analysis indicated an OGIP volume of 45.8 BCF. The condensate yield was approximately 7.7 STB/MMSCF with a gravity of 41º API.

Geological data suggest a uniform GWC across the entire segment and W2 was completed with a 50 ft true vertical depth stand-off from the original GWC located on the flank of the structure.

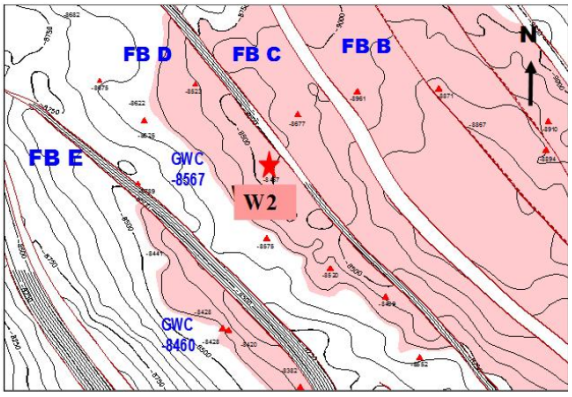

Figure 4. Depth Structure Map for R8 Showing W2 in FB D

3. Pressure Transient Analysis – W1

Both wells have permanent bottom-hole pressure (BHP) and temperature (BHT) gauges. As a result, real time measurements are recorded and can be retrieved simultaneously. All measurements are recorded directly onto a Honeywell Process Historian Database (PHD) server which can then be retrieved and imported into Excel. For the PBU analysis, the following parameters were recovered for each well: date, time, gas rate and bottom-hole pressure. It was also necessary to acquire sufficient rate and pressure history, prior to the build-up. Since pressure changes most rapidly at early time, it is important to determine the exact time of shut in after the flow period. Thus data were recorded in one second intervals for the first two days of each test, and then 15 seconds after that. Also since logarithmic presentations tend to hide errors at late time, and emphasize them at early time, it is important to be cautious with early time buildup data.

The commercial software package used for the pressure analysis was Pression Interpretation d'Essais des puits (PIE) which is French for "pressure analysis of well tests," (Well Test Solutions, 1997). The PIE well-test analysis program is capable of analysing build-up, draw-down and multi-well interference test data. The program can also be used to analyse a test with an arbitrary rate and pressure history and to design well-tests. Analytic type-curve models for specific well and reservoir configurations can be used to analyse test data.

3.1 Time Lapsed Derivative Plots

Figure 5 shows the full pressure and rate history for W1, located in the R7 sand of Fault Block 'D'. The three pressure buildup (PBU) tests conducted over the life of the well i.e. PBU 1, PBU 2 and PBU 3, are also highlighted on this figure, and were conducted at times, recorded from the start of production of 4,811 hrs (June 2007), 11,301 hrs (Feb 2008) and 16,325 hrs (September 2008) respectively.

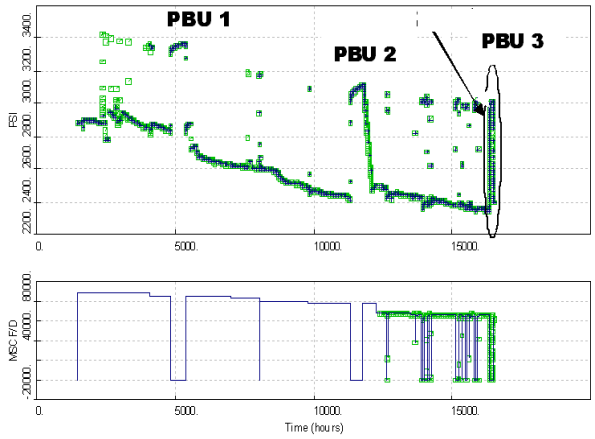

Figure 5. Pressure and Rate History for W1

Each PBU data set was imported into the commercially available pressure analysis software package (Well Test Solutions, 1997), and the composite derivative plot for the three tests are presented in Figure 6 (see Appendix A). This plot, which presents both the pseudopressure drop and pseudopressuretime derivative as a function of elapsed pseudotime for each of the tests (Horne, 1995), allowed one to visually ascertain changes in well and reservoir performance; thus providing for initial qualitative interpretation of the data.

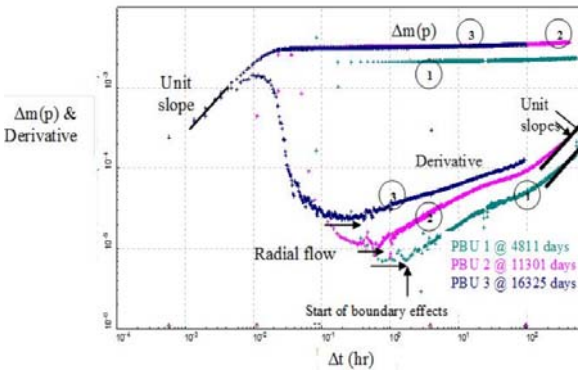

Figure 6. W1 – Derivative Plots for PBU 1, PBU 2 and PBU 3

On the composite log-log plot, the unit slope is observed in the early time region on all plots and is indicative of wellbore storage. On each of the pseudopressuretime derivative plots, the unit slope plus the 'hump' plot indicates wellbore damage, turbulence and inertia effects (i.e. positive skin), while the flat region observed on each derivative plot at intermediate time is indicative of infinite acting radial flow. In addition, the steep transition drop away from the early time wellbore storage unit slope is also characteristic of inertial-turbulent or non-Darcy skin (Horne, 1995; Jemmott et al., 2008; EPS, 2009). Finally, beyond the middle time region, all derivative plots slope upwards indicative of late time boundary effects.

A closer look at the pseudopressuretime derivative plots reveal that the time to the end of radial flow, and start of boundary response, is progressively shorter with each subsequent test. The boundary thus appears not fixed but appears to have moved closer to the well bore region with each successive test. This suggests that the boundary effect observed is not due to a linear barrier/fault, but rather a mobile fluid contact, which in this case is the gas/water contact for the R7 sand (Chen et al., 1996; Dahroug et al., 2005). Further analysis indicated that there is the development of a unit slope in late time for PBU 1 and PBU 2, which is characteristic of edge aquifer systems and which is supported by the geological data.

Gas reservoirs with edgewater drives, such as this reservoir, can be viewed as a composite reservoir with an outer zone of water, and an inner zone of gas (Chen et al., 1996; Dahroug et al., 2005). The mobility ratio between gas and water may be defined as

$$M = (k/\mu)_w / (k/\mu)_g$$

where M = mobility ratio, k = permeability (md), μ = viscosity (cp), w = water and g = gas.

For this reservoir, the gas viscosity is approximately 0.02 cp at reservoir conditions. Assuming a water viscosity at reservoir conditions of approximately 0.5 cp, and that k_w is approximately equal to k_g, then the gas is approximately 25 times more mobile than the water. Thus before water influx becomes dominant, the water behaves like an impermeable medium, and therefore a pseudo-steady state condition can exist in the inner gas zone.

3.2 Type Curve Matching - PBU 3

Figure 7 shows the pressure and rate history PBU 3. This test was conducted at a time of 16,325 hrs in the life of the well. The log-log plot of the extended PBU response for Test # 3 is shown in Figure 8 and pertinent well data are given in Table 1.

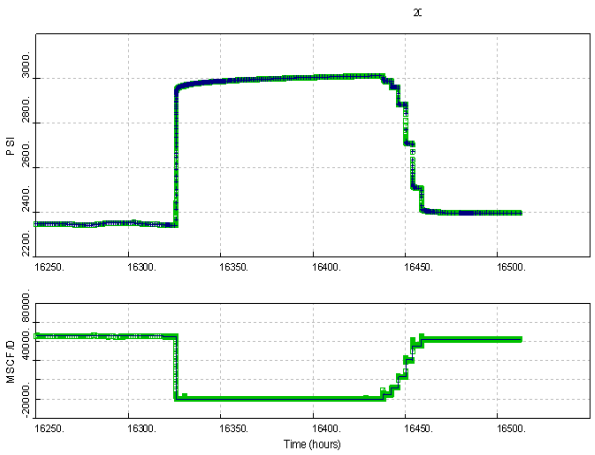

Figure 7. Pressure and Rate History during Pressure Buildup Test # 3 (PBU 3) for W1

Table 1. Fluid Properties for the R7 Reservoir in Fault Block 'D' (FBD)

Gas viscosity @2925 PSI	0.018 CP
Gas viscosity @3400 PSI	0.020 CP
Gas compressibility @3400 PSI	0.25E-03 1/PSI
Water compressibility	0.50E-05 1/PSI
Porosity	24 %
Water saturation	26.4 %
Net thickness	132.3 FT
Rock compressibility	0.5E-05 1/PSI
Well-bore radius	0.46 FT

Figure 8 shows both the pseudopressure drop and pseudopressuretime derivative as a function of elapsed pseudotime. The unit slope is observed in the early time region on this plot and is indicative of wellbore storage. The unit slope plus the hump on the derivative plot is also indicative of a damaged well (i.e. positive skin). The flat region observed on the derivative plot at intermediate time is indicative of infinite acting radial flow. Beyond the middle time region, the derivative slopes upwards indicative of boundary effects.

For the type curve matching, W1 was assumed vertical. Available geological data indicate that this well is the only producer from the R7 sand in Fault Block 'D', and the depth structure map shows that the reservoir compartment is bounded on either side by NW-SE trending faults. This information was combined with the uniform reservoir description based on the available log data and as such a homogeneous reservoir, radial geometry model with two parallel boundaries was assumed for type curve matching. The best type curve match is also presented on Figure 8.

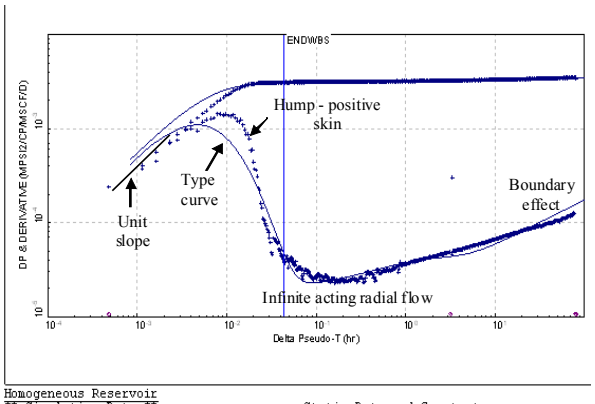

Homogeneous Reservoir

** Simulation Data **		Static-Data and Constants	
well. storage	= 0.020000 BBLS/PSI	Volume-Factor	= 0.5870 RB/MSCF
Skin(darcy)	= 59.103	Thickness	= 132.3 FEET
permeability	= 135.96 MD	Viscosity	= 0.01970 CP
Areal Ky/Kx	= 0.10000	Total Compress	= 0.0001462 1/PSI
Perm-Thickness	= 17981. MD-FEET	Rate	= 64980. MSCF/D
Turbulence	= 0. 1/MSCF/D	Storivity	= 0.004639 FEET/PSI
+x boundary	= 300. FEET (1.00)	Diffusivity	= 51880. FEET^2/HR
-x boundary	= 1450. FEET (1.00)	Gauge Depth	= 8222. FEET
Initial Press.	= 3652.67 PSI	Perf. Depth	= 8498. FEET
Skin(darcy)+DQ	= 59.103	Datum Depth	= N/A FEET
Smoothing Coef	= 0.,0.	Analysis-Data	ID: GAU005

Figure 8. Vertical, Homogeneous, Radial with Two Parallel Boundaries Type Curve for W1

The permeability thickness computed with this model was 17981 mD-feet and based on a net reservoir thickness of 132 ft from available reservoir petrophysics, the permeability was estimated at 136 mD. The total skin (mechanical and Non-Darcy) was also estimated at 59.

3.3 W1 Production Data

Production data for W1 are presented in Figure 9. It shows an initial production high of approximately 100 MMSCF/D which then declined slowly until water breakthrough in September 2008. Thereafter, the well's gas production rate declined sharply to 40 MMSCF/D. At January 2011, the gas production rate was 14 MMSCF/D, the condensate production rate was 58 STB/D, and the water production rate (which increased steadily after breakthrough), was 3800 STB/D.

Figure 10 shows that the cumulative production from W1 at the end of January 2011 was 61 BCF of gas, 0.55 MMSTB of condensate and 2 MMSTB of water. The gas produced accounted for 57% of the OGIP volume generated from the geological model.

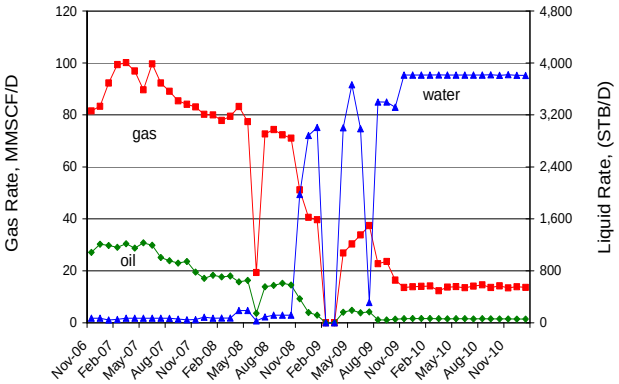

Figure 9. Well Test Data for W1

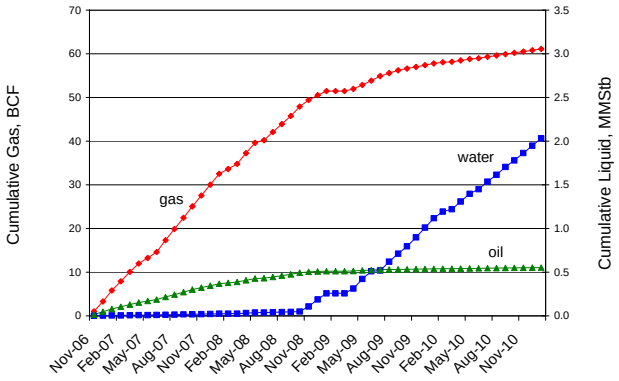

Figure 10. Cumulative Production data for W1

3.4 Residual Water Saturations

The residual saturation tool (RST) is a pulsed neutron tool which is used to determine water saturation in the logged interval. In 2008, the RST was used to determine the resistivity across the producing interval in W1. Water saturations (S_w) were calculated, and subsequently compared to original RST data obtained previously in 2006 when the well was completed.

Figure 11 shows the comparison between the two logs. Both logs are similar except for an approximate 10% increase in S_w in the 2008 log across the bottom half of the section. Of particular importance is that vertical water migration of the GWC is not visible, suggesting that the increase in S_w is due to an edge drive mechanism. The RST data thus led to improved reservoir understanding by confirming the reservoir drive mechanism.

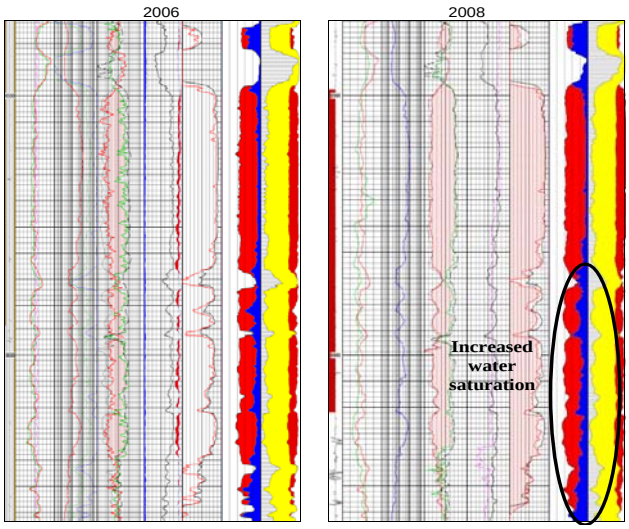

Figure 11. Comparison of Residual Saturation Tool (RST) data for W1

4. Pressure Transient Analysis – W2

4.1 Time Lapsed Derivative Plots

Figure 12 shows the full pressure and rate history for W2, located in the R8 sand of Fault Block 'D'. The three pressure buildup (PBU) tests conducted over the life of the well i.e. PBU 1, PBU 2 and PBU 3, are also highlighted on this figure, and were conducted at times of 585 hrs (June 2007), 6,062 hrs (February 2008), and 11,220 hrs (September 2008) respectively. The composite derivative plot for the three tests is presented in Figure 13.

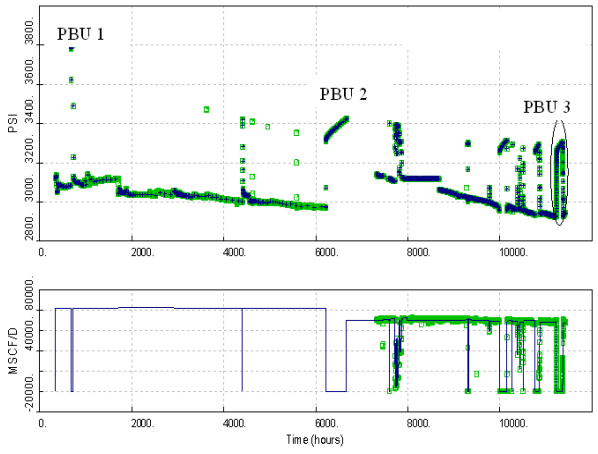

Figure 12. Pressure and Rate History for W2

As occurred for W1, the unit slope is observed in the early time region on all plots and is indicative of wellbore storage. Also at early time, the unit slope plus the hump on each derivative plot is indicative of a damaged well (i.e. positive skin), while the flat regions observed on each derivative plot at intermediate time is indicative of infinite acting radial flow. Beyond the middle time region, all derivative plots slope upwards indicative of late time boundary effects.

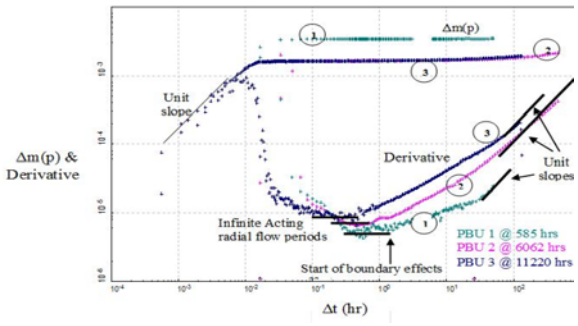

Figure 13. W2 – Derivative Plots for PBU 1, PBU 2 and PBU 3

A closer look at the pseudopressuretime derivative plots reveals that the time to the end of radial flow and start of boundary response is progressively shorter with each subsequent test as was the case with W1. The boundary thus appeared not fixed but to have moved closer to the near well bore region with each successive test. This suggests that the boundary effect observed is not due to a linear barrier/fault, but rather a mobile fluid contact, which in this case is the gas/water contact in the R8 sand. Further analysis indicated that there is the development of a unit slope at late times for PBU 1, PBU2 and PBU 3, which is characteristic of edge aquifer systems (Chen et al., 1996).

4.2 Type Curve Matching - PBU 3

Figure 14 shows the pressure and rate history PBU 3. This test was conducted at a time of 11,220 hrs in the life of the well. The log-log plot of the extended PBU response for Test # 3 is shown in Figure 15.

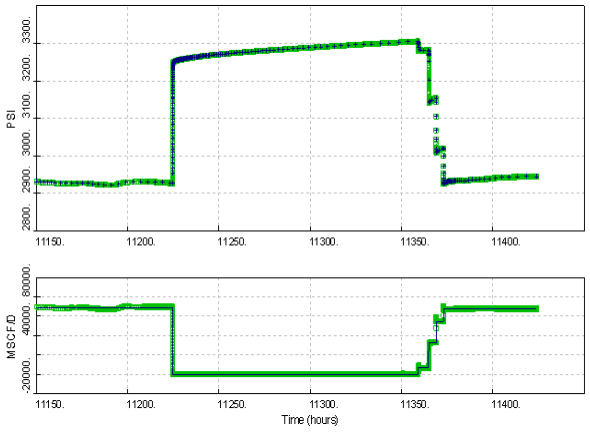

Figure 14. Pressure and Rate History during Pressure Buildup Test # 3 (PBU 3) for W2

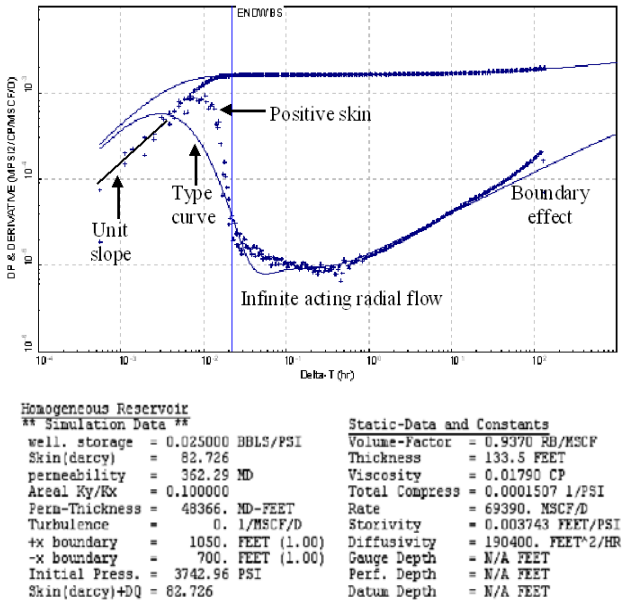

Figure 15. Vertical, Homogeneous, Radial with Two Parallel Boundaries Type Curve for W2

This plot shows both the pseudopressure drop and pseudopressuretime derivative as a function of elapsed pseudotime. The unit slope is observed in the early time region on these plots and is indicative of wellbore storage. The unit slope plus the hump on the derivative plot is also indicative of a damaged well (i.e. positive skin). The flat region observed on the derivative plot at intermediate time is indicative of infinite acting radial flow. Beyond the middle time region, the derivative slopes upwards indicative of boundary effects. Additional fluid properties for the reservoir are listed in Table 2.

Table 2. Fluid Properties for the R8 Reservoir in Fault Block 'D' (FBD).

Gas viscosity @2925 PSI	0.018 CP
Gas viscosity @3400 PSI	0.021 CP
Gas compressibility @3400 PSI	0.2E-03 1/PSI
Water compressibility	0.5E-05 1/PSI
Porosity	18.6%
Water saturation	28.2%
Net thickness	133.5 FT
Rock compressibility	0.5E-05 1/PSI
Well-bore radius	0.46 FT

Available geological data indicated that this well is the only producer in Fault Block 'D' and the depth structure map shows this as a single reservoir compartment bounded on either side by NW-SE trending faults. For the type curve matching, this information was combined with the uniform reservoir description based on the available log data and as such a homogeneous reservoir, radial geometry model with two parallel boundaries was assumed for the match. The best type curve match is also indicated on Figure 15. The reservoir permeability was found to be 362 mD, using a net reservoir thickness of 133 feet and the model-simulated permeability-thickness of 48,366 mD-feet. The total skin (due to near wellbore damage, partial penetration and non-Darcy flow) was estimated at 83.

4.3 W2 Production Data

Production data for W2 are presented in Figure 16. It shows an initial production high of approximately 80 MMSCF/D which then declined slowly until water breakthrough in September 2009. Thereafter, the well's gas production rate declined sharply to 40 MMSCF/D. In November 2009, the well stopped producing after the water production rate had increased to 2700 STB/D.

Figure 17 shows the cumulative production from W2. Cumulative gas, condensate and water production were 42 BCF of gas, 0.2 MMSTB of condensate and 0.1 MMSTB of water. The gas produced accounted for approximately 90% of the OGIP volume generated from the geological model.

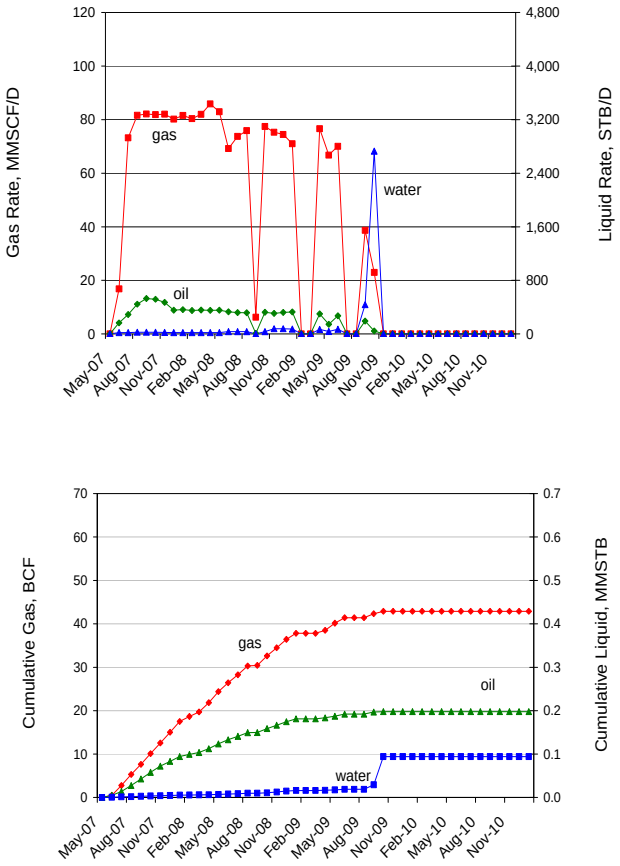

Figure 17. Cumulative Production data for W2

5. Discussion

Although W1 and W2 were completed in separate reservoirs, their responses from pressure transient testing were similar. For W1, while water breakthrough did not occur until November 2008 (11301 hrs), from as early as February 2008 (11301 hrs), i.e. at the time of the second pressure buildup test, one could have confirmed that the late time boundary was 'mobile,' and associated with the encroachment of the aquifer in the R7 sand of Fault Block 'D.' Similarly for W2, from as early as February 2008 (6062 hrs), when the second buildup was analysed, water encroachment could have been confirmed.

With an encroaching aquifer, there is always uncertainty as to how much gas can be produced from the reservoir before the well can no longer lift the reservoir fluids. This is due to a higher fluid density with increasing liquids-to-gas ratios. As seen in both wells, the onset of the sharp increase in water production was accompanied by an almost 50% decline in gas production rates. Even further, in the case of W2, the well died shortly after. Accompanied with the latter is the risk of leaving reserves behind and this is confirmed by the significant difference in recoveries from the R7 and R8 sands of Fault Block 'D.'

The significance of pressure surveillance is thus demonstrated and allows one to plan for expected abrupt changes in production by the early identification of water drive reservoirs.

6. Conclusions

Analysis of 'time-lapsed' pressure transient data from two (2) wells indicated boundary effects as a result of the mobility contrast between gas at the reservoir boundaries, and water in encroaching aquifers. Water movement towards the wells were interpreted from the progressively earlier time at which the boundary response was observed in successive buildup tests.

The above mentioned phenomena was validated by the presence of water-legs based on the geological data, increasing water saturation in the reservoir based on data form the Reservoir Saturation Tool, and a sharp increase in water production rates from both wells. Furthermore, this example illustrated the successful integration of surveillance and geological data to better understand reservoir performance and to identify new wells and recompletion opportunities.

Appendix A:

I. Real Gas Pseudopressure

For analysis of gas well test, since gas properties are strong functions of pressure, the governing equations for slightly compressible flow are modified by the introduction of the **real gas pseudo pressure** variable defined as:

$$m(p) = 2\int_{p_b}^{p} \frac{p}{\mu z} dp \qquad (1)$$

P_b is an arbitrary base pressure, usually at the lowest end of the range of pressures of interest during the test.

To calculate pseudo pressures, numerical integration may be done using the following equation:

$$m(p) = 2\sum_{i=2}^{n} \frac{1}{2}\left[\left(\frac{p}{\mu z}\right)_{i-1} + \left(\frac{p}{\mu z}\right)_{i}\right](p_i - p_{i-1}) \qquad (2)$$

The gas viscosity data for W1 are presented graphically in Figure A1 and the corresponding pseudopressure data for W1 are given in Table A1.

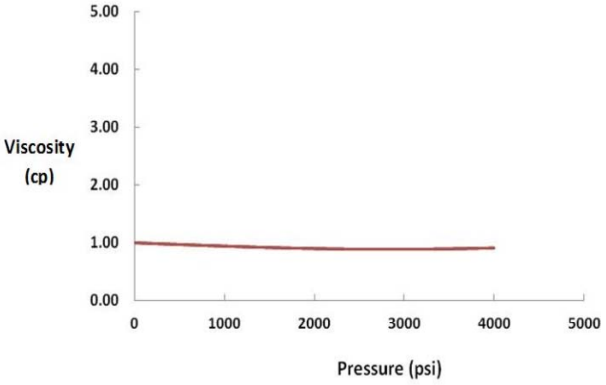

Figure A1. Viscosity as a Function of Pressure for W1

Table A1. Pseudopressure Data for W1

p (psia)	μ (cp)	z	2p/(μz) (psi/cp)	Area	m(p) (psi²/cp)
15	0.012	1.00	2451		
200	0.012	0.99	32812	3267141	3267141
400	0.013	0.98	64493	9730517	12997658
600	0.013	0.96	95111	15960477	28958135
800	0.013	0.95	124709	21982020	50940155
1000	0.014	0.94	153297	27800615	78740770
1200	0.014	0.93	180862	33415938	112156707
1400	0.015	0.92	207363	38822532	150979239
1600	0.015	0.91	232745	44010794	194990033
1800	0.016	0.90	256937	48968128	243958161
2000	0.016	0.90	279865	53680187	297638348
2200	0.016	0.89	301456	58132153	355770501
2400	0.017	0.89	321643	62309952	418080453
2600	0.017	0.88	340370	66201354	484281807
2800	0.018	0.88	357598	69796884	554078691
3000	0.018	0.88	373307	73090498	627169190
3200	0.019	0.89	387493	76079993	703249183
3400	0.019	0.89	400178	78767152	782016335
3600	0.020	0.89	411398	81157645	863173980
3800	0.020	0.90	421209	83260714	946434695
4000	0.021	0.91	429678	85088706	1031523401

II. The Composite Log-Log Plot

Well test analysis makes considerable use of graphical presentations. These presentations are examined to correctly identify the different characteristic flow periods occurring during the test. The composite log-log plot for slightly compressible fluids (Bourdet et al., 1983) provides a simultaneous presentation of *pressure change* vs *delta-time*

and the *pressure derivative* versus *delta-time.* The derivative is the slope of the data when plotted on a semi-log plot i.e.

$$Der = \frac{(\Delta p)}{\Delta \ln(t)} \tag{3}$$

The advantage of the composite plot is that it allows one to display in a single graph, several characteristics that would otherwise require different plots.

Wellbore storage

In a buildup test, when a well is shut in at the surface, fluid continues to enter the wellbore at the sand face. After some time, fluid flow into the wellbore (i.e. at the sandface) is negligible, and the pressure response follows that of the formation.

Early time pressure data is affected by afterflow which is one type of Wellbore Storage (Fekete Associates Inc., 2007). During this period, the pressure response follows the equation

$$\Delta m(p) = 2348\frac{qTt_a}{\mu_g C_s} \tag{4}$$

and

$$\log(\Delta m(p)) = \log\left(2348\frac{qT}{\mu_g C_s}\right) + \log(t_a) \tag{5}$$

This equation is linear with respect to time and a plot of $\log(\Delta m(p)) vs \log(t)$ will have a slope equal to one. The derivative of Equation (4) is

$$Der = 2348\Delta t_a \frac{qT}{\mu_{gi} C_s} \tag{6}$$

and

$$\log(Der) = \log\left(2348\frac{qT}{\mu_{gi} C_s}\right) + \log(\Delta t_a) \tag{7}$$

This equation is linear with time, thus the derivative of wellbore storage data falls on a straight line with slope equal to 1. The purpose of analysing wellbore storage is to determine the wellbore storage coefficient C_s, and to determine when afterflow ends and reservoir dominated data begins.

Radial Analysis

Radial flow is a flow regime that occurs in the middle time (infinite-acting) region, before the occurrence of boundary effects. The purpose of analysing radial flow is to determine permeability-k and apparent skin-s'. For a gas well

$$m(p_i) - m(p_{wf}) = 1.632*10^6 \frac{q_g T}{kh}\left[\log\frac{kt_a}{\phi\mu_{gi}c_{ti}r_w^2} - 3.23 + 0.87s'\right] \tag{8}$$

Where $s' = s + Dq$ i.e. skin due wellbore damage (s), and turbulence and inertia effects (Dq). Equation (8) can also be written as

$$m(p_i) - m(p_{wf}) = 1.632*10^6 \frac{q_g T}{kh}[\log(t_a)] + 1.632*10^6 \frac{q_g T}{kh}\left[\log\frac{k}{\phi\mu_{gi}c_{ti}r_w^2} - 3.23 + 0.87s'\right] \tag{9}$$

The derivative of equation (9) with respect to the natural logarithm of time is

$$Der = 7.088*10^5 \frac{q_g T}{kh} = Const \tag{10}$$

The derivative does not vary with time, and as a result the derivative of radial flow data falls on a horizontal straight line, with slope equal to zero.

Linear Channel

This is a flow regime that exists in long, narrow reservoirs. It occurs after radial flow, in the transition between the middle time region and the late time region, and when the radius of investigation has reached the sides of the channel. During this period, the pressure response follows the equation

$$m(p_{wf}) = m(p_i) - 8.157*10^4 \frac{q_g T}{hW}\left[\frac{\sqrt{t_a}}{\sqrt{k\phi\mu_{gi}c_{ti}}}\right] \tag{11}$$

and

$$\log(\Delta m(p)) = \log\left(8.157*10^4 \frac{q_g T}{hW}\frac{1}{\sqrt{k\phi\mu_{gi}c_{ti}}}\right) + \frac{1}{2}\log(t_a) \tag{12}$$

Equation (12) indicates that a plot of $\log(\Delta m(p)) vs \log(t_a)$ will have a slope equal to 1/2. The derivative of eqn (11) with respect to the natural logarithm of time is

$$Der = \frac{1}{2}8.157*10^4 \frac{q_g T}{hW}\left[\frac{1}{\sqrt{k\phi\mu_{gi}c_{ti}}}\sqrt{t_a}\right] \tag{13}$$

and

$$\log(Der) = \log\left(\frac{1}{2}8.157*10^4 \frac{q_g T}{hW}\frac{1}{\sqrt{k\phi\mu_{gi}c_{ti}}}\right) + \log\left(\sqrt{t_a}\right) \tag{14}$$

A plot of log(Der) vs $\log(t_a)$ will have a slope of ½.

Pseudosteady State Analysis

Pseudosteady flow occurs in a bounded reservoir, after the pressure transient has reached all the boundaries of the reservoir. This analysis allows one to determine reservoir pore volume. During this period, the pressure response follows the equation:

$$m(p_{wf}) = m(p_i) - 1.417*10^6 \frac{q_g T}{kh}\left[\frac{0.00052kt_a}{\phi\mu_{gi}c_{ti}r_e^2} + \ln\left(\frac{r_e}{r_w}\right) - \frac{3}{4} + s'\right] \tag{15}$$

where

$$Der = \frac{2348q_g T\Delta t_a}{Ah\phi\mu_{gi}c_{ti}} \tag{16}$$

and

$$Log(Der) = \log\left(\frac{2348q_g T}{Ah\phi\mu_{gi}c_{ti}}\right) + \log(\Delta t_a) \tag{17}$$

$Log(Der) vs \log(t)$ will therefore plot as a straight line with slope equal to one. For a circular reservoir, the drainage area is proportional to r_e^2. Most reservoirs are however irregular in shape and the well is not always in the centre of the reservoir.

When reservoir pressure falls below the initial reservoir pressure (p_i), the late time or pseudosteady state flow equation (Lee et al., 1996) can also be written as:

$$p_p(\bar{p}) - p_p(p_{wf}) = \left(\frac{1.422 * 10^6 qT}{k_g h} * \left[1.151 \log\left(\frac{10.06A}{C_A r_w^2} \right) - \frac{3}{4} + s + Dq \right] \right) \quad (18)$$

Where $\bar{p}$ is the current drainage area pressure. C_A is a geometric shape factor which is characteristic of the system shape and the well location and has been determined for a variety of drainage areas (Dietz, 1965). The shape of the log-log and derivative plots will therefore be dependent on the system shape, the well location and drainage area.

Addition models such as that for fracture flow, and reservoirs with single and right-angle faults are presented in the literature (GrinGarten, 2001; Fekete Associates Inc., 2007; Stewart, 2009).

References:

Bourdet, D., Whittle, T.M., Douglas, A.A. and Pirard, Y-M. (1993), "A new set of type curves simplifies well test analysis," *World Oil*, May, pp.95-106.

Chen, C.C., Chu, W.C., and Sadighi, S. (1996), "Pressure-transient testing of gas reservoirs with edge-water drive", Society of Petroleum Engineers Formation Evaluation, December, pp.251-256

Dahroug, A.M., Baily, J.W. and Zheng, S.Y. (2005), "The application of transient pressure testing to track phase boundaries during production - a one well case study from UKSC", *Proceedings of The Society of Petroleum Engineers Europec/European Association of Geoscientist & Engineers Annual Conference* (SPE94446), Madrid, Spain, pp.1-17.

Dietz, D.N. (1965), "Determination of average reservoir pressure from build-up surveys", *Journal of Petroleum Technology*, August, pp. 995-959

EPS (2009), *Welltest Analysis*, Edinburgh Petroleum Services Limited, Weatherford, Edinburgh, Scotland.

Fekete Associates Inc. (2007), *FAST WellTest Technical Documentation*, Fekete Associates, available at: http://www.fekete.com/software/welltest/media/webhelp/index.htm [Accessed Nov 14 2011]

GrinGarten, A.C. (2001), *Well Test Analysis*, Course Notes -SPE Technology Update Lecture Series, April 11, Society of Petroleum Engineers Trinidad and Tobago Section

Horne, R.N. (1995), *Modern Well Test Analysis – A Computer Aided Approach*, Second Edition, Petroway, Inc., Palo Alto, California, USA (ISBN 0-9626992-1-7)

Jemmott, S. (2005), "Reservoir surveillance in gas reservoirs offshore Trinidad", *Proceedings of The Society of Petroleum Engineers Latin American and Caribbean Petroleum Engineering Conference* (SPE94820), 20-23 June, Rio de Janeiro, Brazil, pp.1-9.

Jemmott, S.T., Baksh, K. and Jones, J. (2008), "Initial surveillance in the Cannonball field: design, implementation, and interpretation", *Proceedings of The CIPC/ Society of Petroleum Engineers Gas Technology Symposium* (SPE114257), 16-19 June, Calgary, Alberta, Canada, pp.1-14

Lee, J. and Wattenbarger, R.A. (1996), *Gas Reservoir Engineering,* SPE Textbook Series Vol.5 (ISBN 1-55563-073-1), Society of Petroleum Engineers. Richardson, Texas

Lumsden, P.J., Balgobin, C.J., Bodnar, D., Brayshaw, A.C., Dyer, B.L., Gainski, M., Hennington, E.R., Burch, T.K. Farmer, C.L. and Saldana, M.A. (2002), "The Kapok field - a step change for Trinidad gas developments", *Proceedings of The SPE Gas Technology Symposium* (SPE, 75670), 30 April-2 May, Calgary, Alberta, Canada, pp.1-10

Mohammed, S. (2010), *Reservoir Management of an Offshore Water Driven Gas Field Through Pressure Transient Analysis*, Report submitted in fulfillment of M.Sc. Petroleum Engineering, The University of the West Indies, Trinidad and Tobago, pp 1-132

Samsundar, K., Moosai, R.S. and Chung, R. (2007), "Surveillance planning: the key to managing a mature gas reservoir", *Proceedings of The Society of Petroleum Engineers Latin American & Caribbean Petroleum Engineering Conference* (SPE107279), 15-18 April, Buenos Aires, Argentina, pp.1-7

Stewart, G. (2009), *Welltest Analysis,* Course Notes, Weatherford, Edinburgh Petroleum Services Ltd., Edinburgh

Well Test Solutions (1997), *Pie Well-Test Software*, available at http://welltestsolutions.com/ [Assessed: 7 June October 2011]

Author's Biographical Notes:

Jill Marcelle-De Silva *is a petroleum engineer by profession with 17 years experience in the energy sector at Petrotrin (Trinidad) and later BP Trinidad & Tobago LLC. She holds both B.Sc. and M.Sc. Degrees in Petroleum Engineering from the University of the West Indies (UWI), and an Engineer's Degree in Petroleum Engineering from Stanford University, California. Her professional career involved experience in numerical simulation, risk analysis, enhanced oil recovery, estimation of oil and gas reserves, preparation of long term field management plans, and predicting, monitoring, and optimising the production performance of oil and gas fields. She joined UWI as a lecturer in the Petroleum Engineering Unit in 2000, and has published technical papers on natural gas hydrates, development of thin oil rims, the evaluation of exploration prospects, development of major gas fields and the effects of permeability and wettability heterogeneities on flow in porous media.*

Shireen Mohammed *is a petroleum engineer by profession and is currently employed with BP Trinidad & Tobago LLC. She recently completed the M.Sc. Degree in Petroleum Engineering from the University of the West Indies (UWI).*

■